frontiers | Frontiers in Earth Science

TYPE Original Research
PUBLISHED 30 May 2025
DOI 10.3389/feart.2025.1609857

OPEN ACCESS

EDITED BY
Vasyl Lozynskyi,
Dnipro University of Technology, Ukraine

REVIEWED BY
Volodymyr Falshtynskyi,
National Mining University of Ukraine, Ukraine
Shenguang Fu,
The Pennsylvania State University (PSU), United States

*CORRESPONDENCE
Yiwen Ju,
juyw03@163.com

RECEIVED 11 April 2025
ACCEPTED 19 May 2025
PUBLISHED 30 May 2025

CITATION
Wang P, Ju Y, Ren C, Li G, Xiao L, Wang W, Gao J and Chen R (2025) Effect of pore structure on methane adsorption characteristics in tectonically deformed coals. *Front. Earth Sci.* 13:1609857. doi: 10.3389/feart.2025.1609857

Effect of pore structure on methane adsorption characteristics in tectonically deformed coals

Peng Wang[1], Yiwen Ju[1]*, Chunhui Ren[2], Guofu Li[3], Lei Xiao[1], Wei Wang[1], Jian Gao[1] and Renzhe Chen[1]

[1]National Key Laboratory of Earth System Numerical Modeling and Application, College of Earth and Planetary Sciences, University of Chinese Academy of Sciences, Beijing, China, [2]Qingdong Coal Mine Huaibei Min Co., Ltd., Huaibei, Anhui, China, [3]State Key Lab Coal and Coalbed Methane Comining, Jincheng, China

The regulation of pore structure on methane adsorption and free state in tectonically deformed coals directly affects the efficiency of coalbed methane extraction and coal mine safety. In this paper, we systematically characterised the full-size pore structure of different deformed coals (primary, brittle and ductile) in Huaibei mining area by integrating mercury intrusion, low-temperature nitrogen adsorption, carbon dioxide adsorption and methane isothermal adsorption, quantified the pore dynamics evolution law by combining with the fractal theory, and resolved the adsorption mechanism. The results show that: (1) the coal mainly consists of micropores (17.0–45.9%) and macropores (46.8–76.9%), with fewer mesopores (1.6–7.3%). With the intensification of tectonic deformation, the volume of micropores and macropores increased by 0.013 cm^3/g and 0.097 cm^3/g, respectively, and the specific surface area increased by ~40 m^2/g and <2 m^2/g, respectively. Fractal analysis showed that macroporous complexity (D_1) decreased while microporous complexity (D_3) increased during ductile deformation; (2) microporous parameters (volume, specific surface area) dominated methane adsorption capacity (R^2 > 0.7), while macroporous enlargement (up to 0.108 cm^3/g) exacerbated the risk of free methane enrichment; (3) Brittle deformed coal is suitable for coalbed methane development due to microporous optimisation, while ductile deformed coal requires enhanced gas prevention and control due to free gas enrichment in large pores. The study reveals the dynamic correlation mechanism of 'pore evolution, adsorption/free gas and disaster risk' under the tectonic deformation gradient, which provides theoretical support for the efficient development and safe exploitation of coalbed methane.

KEYWORDS

tectonically deformed coal, pore structure, methane adsorption, coalbed methane, deformation characterization

1 Introduction

Coal bed methane (CBM), primarily composed of methane, is a hydrocarbon gas found in coal seams and represents an important non-conventional energy source

while also being a significant factor contributing to coal and gas outbursts (Moore, 2012; Zhang C. et al., 2019). It primarily exists in a free phase within macropores and fractures, or in an adsorbed state on the surfaces of micropores and mesopores (Zou et al., 2015; Zhang et al., 2018). Due to the multiple tectonic movements experienced by various basins in China, coal seams have undergone varying degrees of tectonic deformation (Pan et al., 2016; Ju et al., 2018; Yu S. et al., 2018), resulting in the extensive development of different types of tectonically deformed coal across the country. Tectonically deformed coal may have formed due to a combination of brittle, shear/transitional, and ductile deformations (Ju et al., 2005), along with the tectonic stresses commonly associated with geological processes. It is widely accepted that brittle deformed coal is linked to high-quality coalbed methane development areas, whereas ductile deformed coal is associated with regions that have a high incidence of coal and gas outbursts (Qu et al., 2017; Song et al., 2017b; Yu et al., 2017; Yuan et al., 2017). Therefore, studying the occurrence of adsorbed and free methane in tectonically deformed coal has significant theoretical and practical implications for coalbed methane production and coal mine safety.

The differences in coal formed under various deformation environments can be attributed to the internal heterogeneity and pore structure, which includes pore size distribution (PSD), pore volume, and specific surface area. These factors significantly influence coalbed methane exploration and the occurrence of gas outbursts (Fu et al., 2009; Yao et al., 2009; Song et al., 2019). Consequently, extensive research has been conducted over the past few decades on the heterogeneity of pore structures in tectonically deformed coal (Li et al., 2012; Xu et al., 2014; Li et al., 2015; Pan et al., 2015; Song et al., 2017a). Recent studies have shown that tectonic deformation has a more significant effect on the evolution of nanopore structure compared to magmatic thermal action (Ju et al., 2005). For example, tectonic stress can significantly increase the total pore volume and change the distribution characteristics of pores at different scales (Liu et al., 2015). Zhu et al. (2020) demonstrated through strain adsorption experiments that micropores, mesopores, and transitional pores predominantly govern the adsorption properties of coal. Analysis of nanopore structures using gas adsorption methods and scanning electron microscopy (SEM) indicates that gas adsorption is more closely related to the specific surface area of the pores than to the mineral composition (Wang et al., 2016; Zhou et al., 2018; Liu et al., 2019). Methane adsorption behavior varies according to pore type; specifically, adsorption in elemental particle pores is influenced by specific surface area (SSA), while adsorption in molecular structure pores depends on pore volume. The relationship between Langmuir volume and pore parameters shows that micropore volume and vitrinite reflectance collectively influence gas adsorption (Moore, 2012; Chen et al., 2017; Li et al., 2023). The micropore filling theory model further quantifies the adsorption characteristics of methane within the pore size range of 0.38–1.5 nm (Hu et al., 2020; Liu et al., 2024; Zhang et al., 2025), and quantitatively differentiates between micropore filling and external surface adsorption (Cheng and Hu, 2021). This theoretical framework integrates molecular dynamics models with multilayer adsorption calculations based on the specific surface area of coal and non-local density functional theory (NLDFT) analyses of pore size distribution. By incorporating molecular dimensions of N_2 and CO_2 and fitting Langmuir models for CH_4 adsorption under high- and low-pressure conditions, the methane adsorption capacity is rigorously validated (Cheng and Hu, 2021; Fu et al., 2023; Hu et al., 2021). Furthermore, while traditional micropore filling theory posits a close match between coal matrix pore channels and CH_4 molecular dimensions, recent studies challenge this paradigm by proposing that stable accommodation of methane within micropores requires a specific equilibrium distance. This distance exhibits a positive correlation with organic matter content in coal (Fu et al., 2024), thereby providing novel insights into pore-composition coupling mechanisms.

Despite extensive research on pore structure and gas adsorption in coal, controversy remains regarding the primary factors affecting methane adsorption capacity. Existing studies predominantly focus on static pore characteristics or the effects of isolated deformation types on coal reservoirs, lacking systematic analysis of the dynamic evolution mechanisms of pore structures under tectonic deformation gradients (e.g., primary coal→brittle→ductile deformed coal). Controversies persist regarding the synergistic roles of micropores and macropores in methane adsorption and free gas storage, while engineering practices lack robust criteria for gas outburst risk classification across differentially deformed coals. To address these gaps, this study integrates mercury intrusion porosimetry (MIP), low-temperature nitrogen adsorption (LTNA), CO_2 adsorption, and methane isothermal adsorption experiments to systematically characterize full-aperture pore structures. Fractal theory is employed to quantify pore complexity, and results are correlated with methane adsorption capacity. Key innovations reveal that tectonic deformation significantly enhances micropore volume and specific surface area while macropores exhibit volumetric expansion but structural simplification, as evidenced by inverse evolutionary patterns in fractal dimensions. Furthermore, micropore parameters strongly correlate with methane adsorption capacity, whereas macropore enlargement promotes free methane accumulation, elevating gas outburst risks. These findings propose brittle deformed coal as a favorable target for CBM exploitation due to optimized micropores, while ductile deformed coal requires enhanced gas hazard mitigation due to macropore-dominated free gas reservoirs, thereby advancing the understanding of the "deformation-pore-adsorption-hazard" dynamic interplay.

2 Samples and experiments

2.1 Samples

The Huaibei mining area is located at the southeastern margin of the North China Plate (Figure 1a) and is influenced by the subduction and collision between the South China and North China Plates, as well as by the subduction of the Pacific Plate. The Carboniferous-Permian coal-bearing strata in the region underwent complex tectonic evolution during the Mesozoic, characterized by a network of east-west and north-northeast trending major faults, resulting in a block faulting structure (Zheng et al., 2021) (Figure 1b). Consequently, the Huaibei mining area has become one of the most severely affected regions in China regarding coal and gas outbursts (Ju et al., 2005; Jiang et al., 2010). Samples were collected from the southeastern Qingdong coal mine in the Huaibei mining area (Figure 1c), where small normal faults oriented NWW,

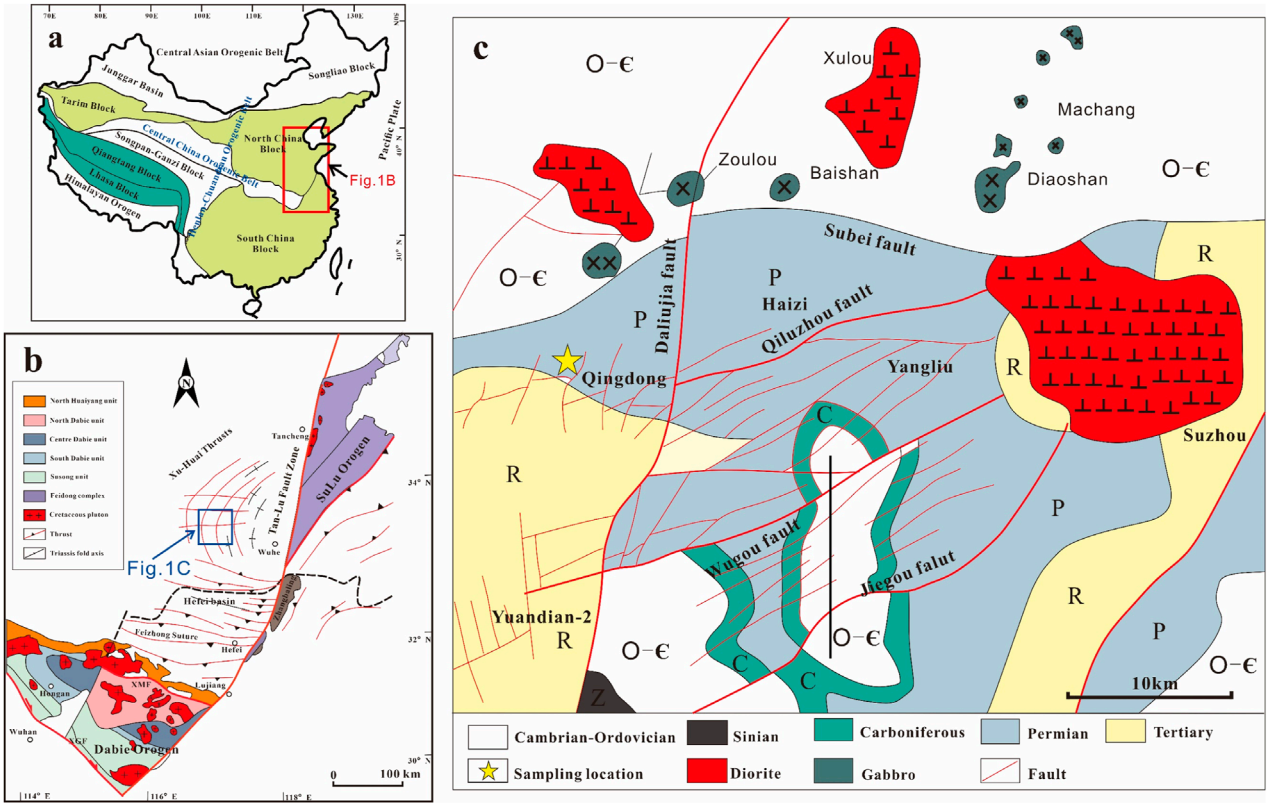

FIGURE 1
(a) Location of the Huaibei mining area in China; **(b)** Tectonic framework of the Huaibei mining area; **(c)** Location of the Qingdong coal mine and surrounding structural lines [Modified from Zheng et al. (2021)].

NNE, and NNW are developed, and various types of tectonically deformed coal are widely present.

The pore structure and adsorption/desorption properties of coal are influenced by various geological factors (Li et al., 2022). To emphasize the effects of tectonic deformation, a rigorous sampling methodology was employed to eliminate the influence of extraneous factors on the results. Sampling points were selected to avoid areas of magmatic intrusion and geological formations, thereby reducing the impact of coal maturity and thermal metamorphism. Tectonically deformed coal and pristine coal samples were collected from the same stratigraphic level within the same region to mitigate the influences of coal formation age and environmental conditions. Samples were obtained from the newly exposed No. 7 coal seam of the Lower Shihezi Formation in the Qingdong coal mine. Based on classification criteria related to deformation characteristics and structure (Ju et al., 2004), five representative samples were chosen to identify the deformation series (brittle, brittle-ductile transitional, and ductile) and the types of tectonically deformed coal. Through the analysis of macro- and micro-deformation structures and characteristics, the coal types were classified as Primary coal (MT01), Granulitic coal (MT02), Scaly coal (MT03), and Mylonite coal (MT04, MT05) (Figure 2).

The coal samples were classified as medium-rank bituminous coals with medium–high volatile content, based on proximate analysis and vitrinite reflectance measurements performed in accordance with national standards GB/T212–2008 and GB/T6948-2008. Analytical results (Table 1) indicate that the maximum vitrinite reflectance ($R_{o,max}$) ranges from 1.23% to 1.34%, while volatile matter content (V_{ad}) varies between 24.51% and 26.32%. The narrow $R_{o,max}$ range and consistent medium metamorphic grade effectively minimize the confounding effects of thermal maturation on pore structure evolution and gas adsorption/desorption behavior. Previous studies have demonstrated that structural stress predominantly governs nanopore development in medium-rank tectonically deformed coals (Wang et al., 2022), establishing a robust foundation for investigating pore structure-controlled adsorption/desorption mechanisms. Consequently, the selection of medium-rank deformed coals as the primary research subject aligns with the objectives of isolating deformation-driven pore dynamics from thermal metamorphic influences.

2.2 Experimental methods

2.2.1 Mercury injection porosimetry

The pore size distribution of materials, particularly mesopores and macropores, is assessed using the mercury injection technique. This method is based on the principle that mercury cannot wet solid surfaces and thus requires external pressure to enter the internal pores of solids (Yu K. et al., 2018). By measuring the volume of

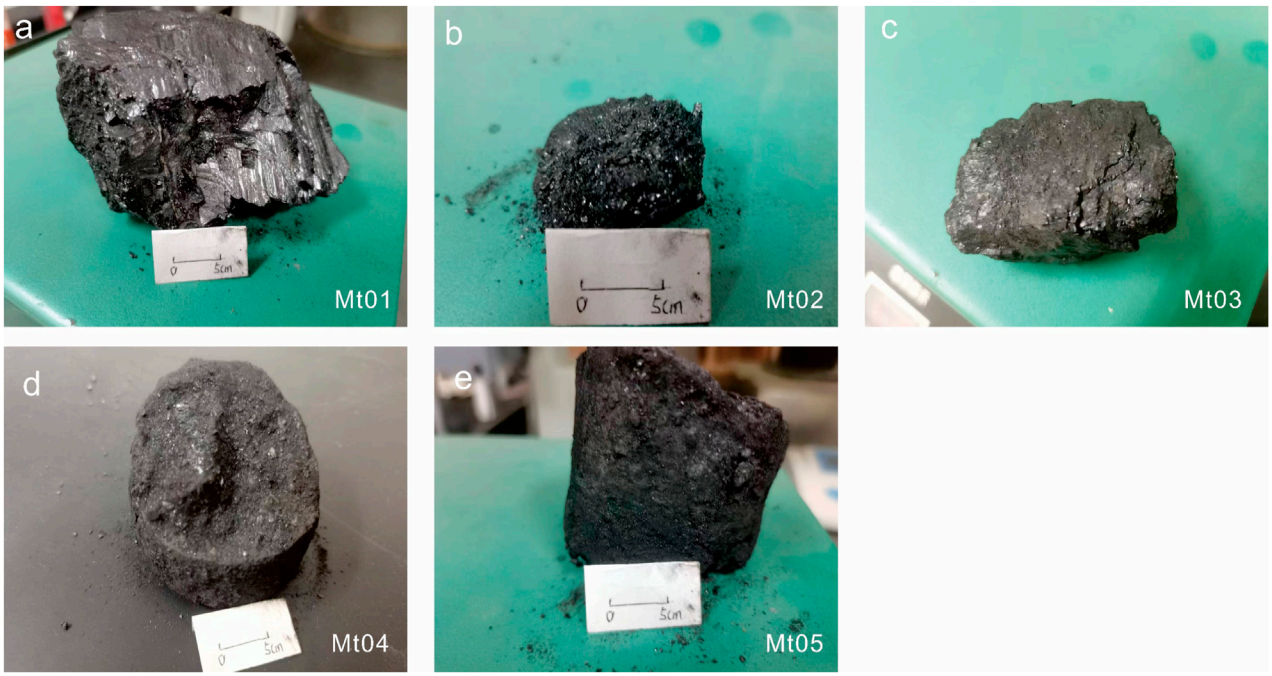

FIGURE 2
Macroscopic structural deformation of coal samples. **(a)**, Primary coal; **(b)**, Granulitic coal; **(c)**, Scaly coal; **(d,e)**, Mylonite coal.

TABLE 1 Basic properties of tectonically deformed coals.

Sample no.	Type	$R_{o,max}$ (%)	M_{ad}	A_{ad}	V_{da}	FC_{ad}	C_{daf}	H_{daf}
MT01	Primary coal	1.23	0.82	21.46	26.32	51.14	86.82	5.10
MT02	Granulitic coal	1.25	0.87	22.37	24.51	52.38	90.56	4.98
MT03	Scaly coal	1.30	0.84	22.44	24.72	52.00	90.75	4.99
MT04	Mylonite coal	1.28	0.96	24.06	25.11	49.87	92.98	5.03
MT05		1.34	0.92	25.15	25.22	48.71	93.28	5.02

Note: $R_{o,max}$, the maximum vitrinite reflectance; ad, air-dry basis; M, moisture; A, ash; V, volatile content; FC, fixed carbon; daf, dry ash-free basis; C,H, contents of carbon, hydrogen.

mercury that infiltrates under various external pressures, the pore volume can be determined. Testing is conducted with the Automatic Porosity Analyzer (Autopore IV 9500 series). Specimens should be coal blocks, measuring between 1 and 2 cm in diameter. Prior to the experiment, these specimens need to be vacuum-dried at 105°C for 5 h. The analyzer operates with an absolute pressure range from 0.55 to 30,000 psia, and it measures pore diameters in the range of 5–39,720 nm.

2.2.2 Low-temperature liquid nitrogen adsorption experiments and carbon dioxide adsorption experiments

The methods of LTNA and carbon dioxide adsorption are mainly used to analyze the specific surface area and pore size distribution of solids by examining gas adsorption behaviors on their surfaces. At constant temperature, the amount of N_2 and CO_2 adsorbed on the pore surfaces shows a specific functional relationship with the relative pressure (P/P_0). The curve that represents the change in adsorption quantity with pressure is known as the adsorption isotherm. In this study, LTNA at 77 K within the relative pressure range of 0.001–0.995 and carbon dioxide adsorption at 273 K within the range of 3×10^{-5}–0.029 were conducted using the Autosorb iQ gas physisorption system (Quantachrome Instruments, USA), in accordance with the National Standards of the People's Republic of China GB/T 21,650.2-2008 and GB/T 21,650.3-2011. Prior to testing, all samples were degassed at 110°C for a minimum of 12 h in the Autosorb iQ degassing station to ensure the removal of moisture and adsorbed gases. The saturation vapor pressure (P_0) for LTNA at 77 K was obtained using a P_0 cell, while a P_0 value of 3.496 MPa was utilized for CO_2 adsorption at 273 K due to its elevated experimental temperature. Using the experimental data, the fundamental pore morphology, including specific surface area

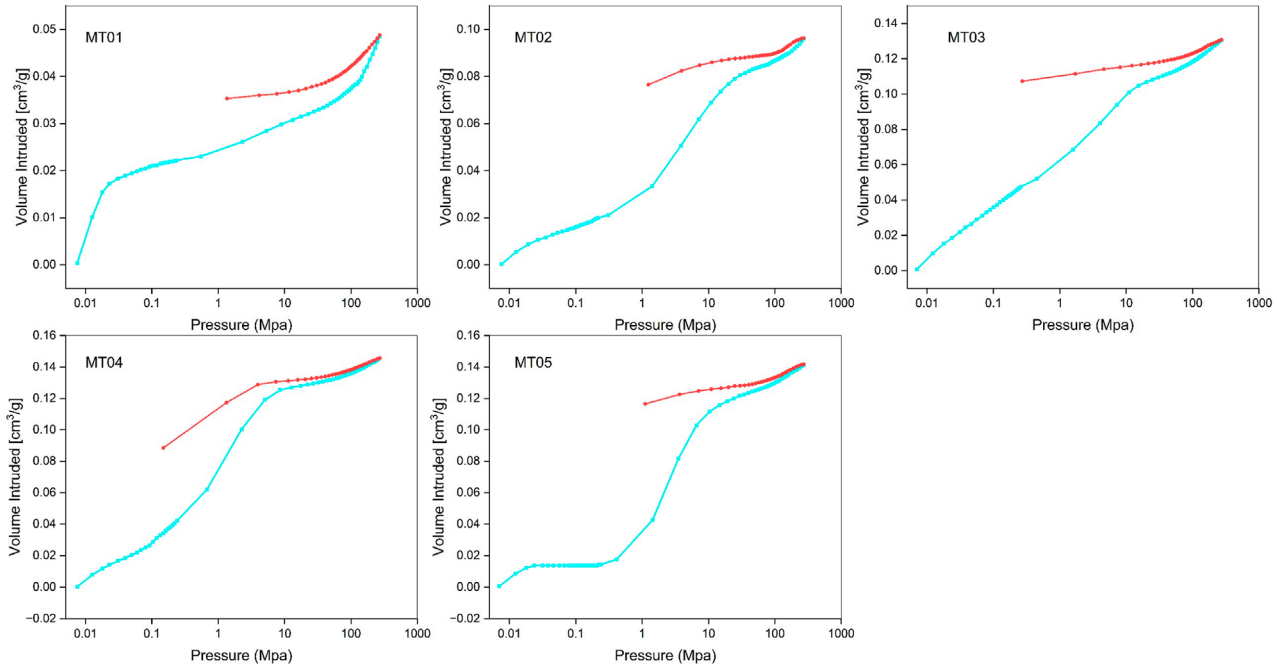

FIGURE 3
Mercury intrusion/withdrawal curves of coal samples.

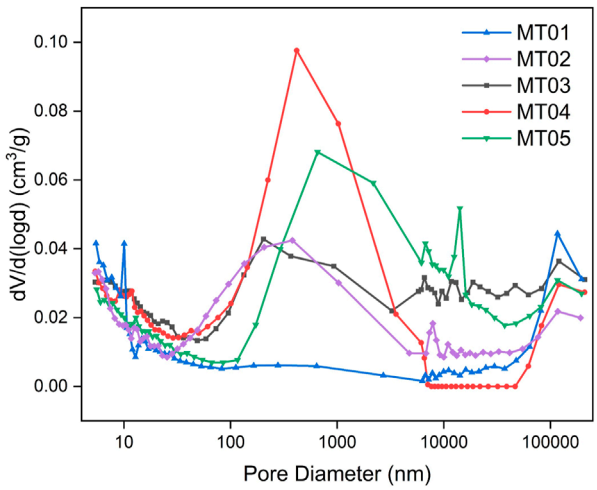

FIGURE 4
PSDs obtained by the MIP analysis of coal samples.

and pore size distribution (PSD), was analyzed through classical methods as well as advanced density functional theory (DFT) (Liu B. et al., 2023; Liu X. F. et al., 2023).

2.2.3 Methane isothermal adsorption experiment

The high-pressure methane isothermal adsorption experiment was conducted in accordance with the national standard GB/T 19,560-2004. The coal samples were first crushed to 60–80 mesh, and after balanced water treatment, they were loaded into the sample tube. Methane adsorption data at different pressure points were obtained at reservoir temperature, and then V_L and P_L were calculated using the equation (He et al., 2020). The methane gas adsorption capacity of coal is generally calculated using the Langmuir equation (Zhang and Liu, 2017): $V=V_LP/(P + P_L)$, where V is the adsorption capacity under pressure P (in cm^3/g), V_L is the Langmuir volume, and P_L is the Langmuir pressure (in MPa). V_L represents the maximum adsorption capacity of coal samples, while P_L is the pressure at half of the maximum adsorption capacity; that is, when $V=V_L/2$, $P=P_L$.

3 Results

3.1 Mercury intrusion porosimetry

The shape of the mercury intrusion/extrusion curves in coal samples is determined by the types, morphology, structure of the pores, and the combinations of pore-fractures (Liu B. et al., 2023). The types of mercury curves for the coal samples are illustrated in Figure 3. All coal samples exhibited distinct S-shaped intrusion curves. The mercury extrusion curve for pristine coal appeared parallel, while the intrusion curve for brittle deformed coal exhibited a negative S shape, with the extrusion curve characterized by a gently concave arc. Mylonite coal exhibited double S shapes, comprising S-shaped intrusion curves and negative S-shaped extrusion curves. Regarding pore connectivity, pores from which mercury is successfully expelled are classified as effective pores, while ineffective pores refer to those within the coal matrix where mercury tends to be retained (Zhang K. Z. et al., 2019). The proportion of effective pores in the coal from this region is relatively

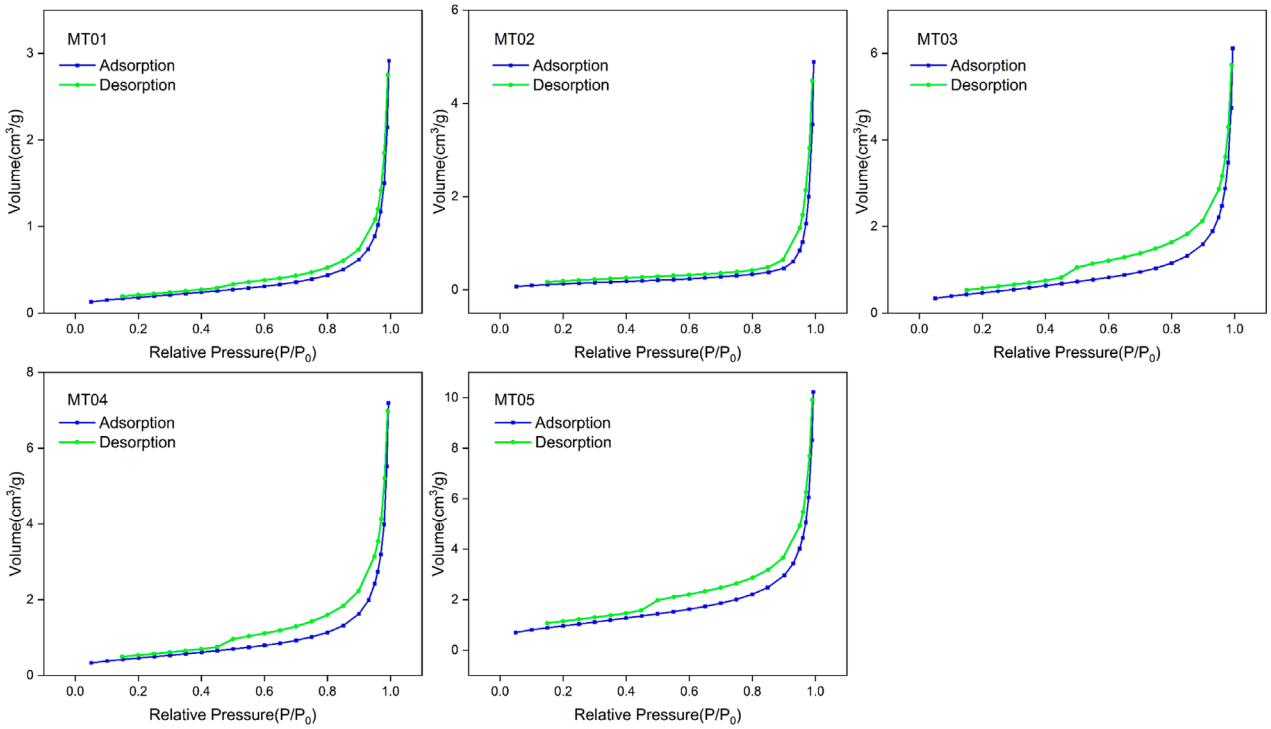

FIGURE 5
Low-temperature N_2 adsorption–desorption curve of coal samples.

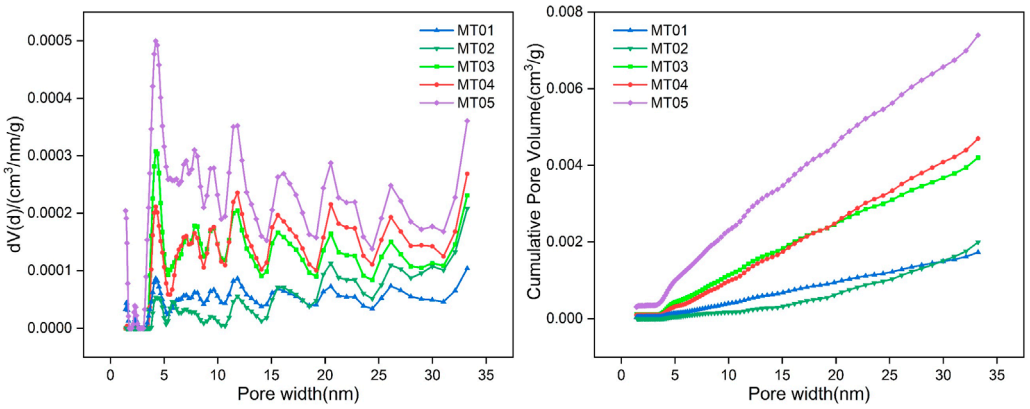

FIGURE 6
PSDs using the LTNA analysis calculated by the DFT model of coal samples.

low, indicating numerous ineffective pathways that hinder gas flow in low-rank coal.

The pore size distribution (PSD) of mesopores and macropores for the five coal samples, measured using the MIP method, is illustrated in Figure 4. All samples exhibit a multimodal distribution, with peak positions primarily around 5-10 nm and 203–654 nm. In pristine coal samples, the pore distribution is primarily in the mesopore range, with very low macropore content and a significant presence of microfractures. In contrast, the PSD peaks for deformed coal samples are predominantly in the macropore range, with ductile deformed coal exhibiting significantly higher macropore content compared to brittle deformed coal. Overall, the development of macropores and microfractures in these coal samples creates additional space for gas migration.

3.2 Low-temperature nitrogen adsorption/desorption

The LTNA isotherms for the samples are illustrated in Figure 5. According to IUPAC classification, the isotherms of the five coal samples are classified as Type IV (Thommes et al., 2015). At low

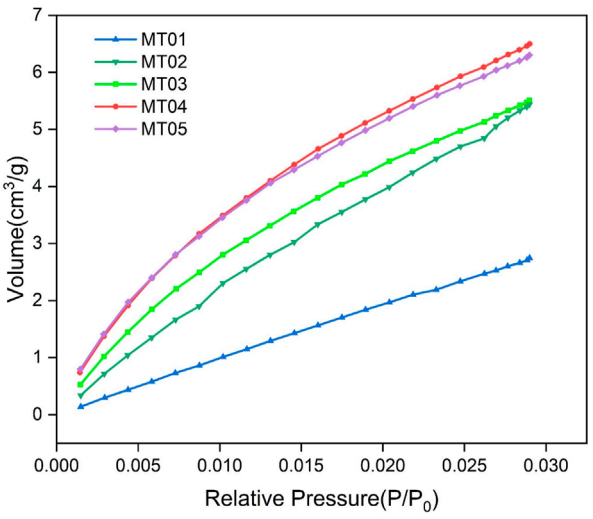

FIGURE 7
CO_2 adsorption isotherms of coal samples.

pressures (P/P_0 < 0.01), the strong adsorption potential created by the overlapping walls of micropores leads to the rapid filling of nitrogen molecules in these regions, resulting in a rapid increase in adsorption capacity. As the relative pressure increases (0.01 < P/P_0 < 0.5), the adsorption curve enters the plateau region, indicating the presence of multilayer adsorption on the surface. When P/P_0 > 0.50, continuous multilayer adsorption occurs in conjunction with capillary condensation. Utilizing the density functional theory (DFT) computational method, pore sizes can be calculated based on the equilibrium gas pressure, allowing for the generation of cumulative or differential PSD curves. After P/P_0 = 0.995, the gas content is gradually reduced to generate the desorption isotherm. The adsorption and desorption curves do not coincide, creating a hysteresis loop. Based on the IUPAC classification of hysteresis loops, the hysteresis loops for samples MT03, MT04, and MT05 are categorized as Type H4. This indicates the probable presence of a substantial number of open and semi-closed pores, as well as slit-like pores within these coal samples (Thommes et al., 2015). The hysteresis loops for samples MT01 and MT02 are classified as Type H3, indicating that these coal samples contain numerous narrow fissure-like pores (Mastalerz et al., 2012).

The pore size distribution (PSD) of LTNA obtained through the DFT method is illustrated in Figure 6. All samples exhibit a multimodal distribution characterized by waveform curves, with the largest peaks occurring between 3 nm and 5 nm. It is evident that while the mesopore size distributions among the different coal samples are similar, significant differences exist in their magnitudes.

3.3 Carbon dioxide adsorption/desorption

Figure 7 illustrates the CO_2 adsorption isotherms for the coal samples. According to the IUPAC classification of adsorption isotherms, the CO_2 adsorption exhibits Type I isotherm curves (Thommes et al., 2015). The gas adsorption capacity increases rapidly with rising relative pressure, followed by a gradual reduction in the rate of increase, indicating that the target coal possesses a well-developed ultra-micropore structure with a broad PSD range.

The pore sizes of the coal samples calculated using the DFT model range from 0.3 to 1.5 nm, as shown in Figure 8. The volume increment curves for all samples exhibit a distinct multimodal distribution, with the most prominent peak at 0.84 nm, along with multiple peaks and minima between 0.4 and 0.7 nm. The cumulative adsorption volume for all samples shows slow growth in the range of 0.24–0.45 nm, with rapid increases observed at 0.4–0.6 nm and 0.8–0.85 nm.

3.4 Methane isotherm adsorption experiment

Figure 9 illustrates the methane isothermal adsorption curves for the Lower Shihezi Formation coal samples. The isothermal adsorption data for all coal samples demonstrate a strong fit with the Langmuir equation, with correlation coefficients exceeding 0.99. The adsorption curves indicate that when the pressure is below 4 MPa, the methane gas adsorption capacity of the samples increases rapidly, exhibiting typical monolayer adsorption characteristics. As the pressure exceeds 8 MPa, the methane gas adsorption capacity of the Lower Shihezi Formation coal samples approaches saturation. The ultimate methane adsorption capacity (V_L) for the five coal samples ranges from 11.66 to 20.37 cm^3/g, with the order of capacity being ductile deformed coal > brittle deformed coal > pristine coal. The Langmuir pressure (P_L) ranges from 3.56 to 3.65 MPa; a higher Langmuir pressure indicates elevated methane gas desorption pressure in coal, facilitating gas desorption and enhancing the development of coalbed methane resources (Yang et al., 2019).

4 Discussion

4.1 Pore structure characteristics

The pores in coal rock span a broad size spectrum and are classified according to the IUPAC guidelines into micropores (<2 nm), mesopores (2–50 nm), and macropores (>50 nm) (Sing et al., 1985). In this study, we integrated results from multiple methods—CO_2 adsorption, LTNA, and MIP—to characterize the complete pore size distribution (PSD). CO_2 adsorption data were utilized to investigate the PSD in the micropore range (<1.5 nm), LTNA data were employed to study the PSD in the micropore to transitional pore range (1.5–35 nm), and MIP data were used to obtain the PSD for pores larger than 35 nm. As shown in Figure 10, the PSD curves for all samples exhibit a multimodal distribution dominated by micropores, while the mesopore distribution displays a waveform characteristic, with a primary stable peak at 35–37 nm.

We statistically analyzed the micropore, mesopore, macropore, total pore volume, and specific surface area of the coal samples using results from CO_2 adsorption, LTNA, and MIP. The pore distributions of all samples exhibit consistent characteristics, as shown in Figure 11. The total pore volume of the coal samples ranges from 0.024 to 0.135 cm^3/g, with pristine coal exhibiting the

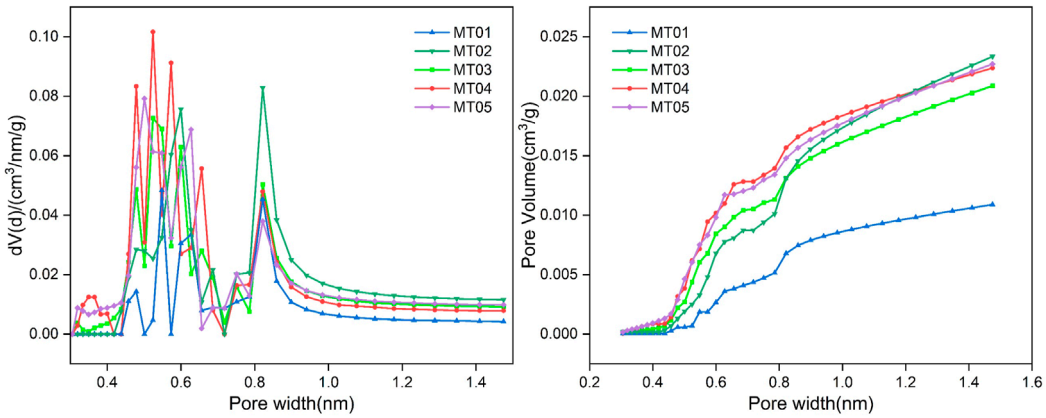

FIGURE 8
PSDs using the carbon dioxide analysis calculated by the DFT model of coal samples.

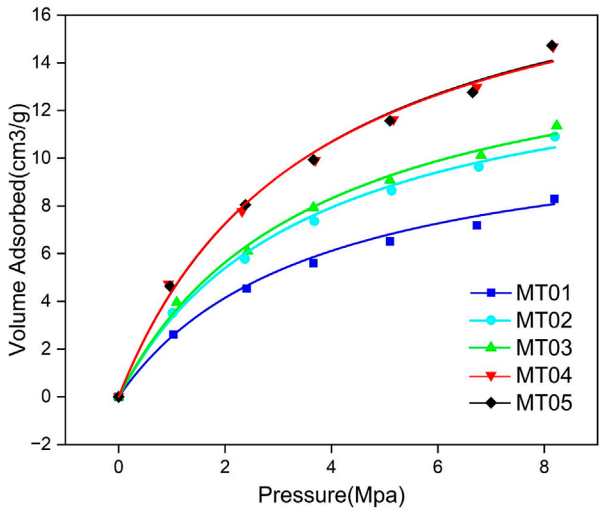

FIGURE 9
Methane isotherm adsorption curve of samples.

lowest pore volume, followed by brittle deformed coal, and ductile deformed coal exhibiting the highest pore volume. The pore volume of tectonically deformed coal is primarily attributed to macropores and micropores, with macropore volumes ranging from 0.011 to 0.108 cm^3/g, accounting for 46.8%–76.9% of the total pore volume. Micropore volumes range from 0.011 to 0.024 cm^3/g, constituting 17.0%–45.9% of the total pore volume, while mesopore content is minimal, representing only 1.6%–7.3% of the total pore volume. With increasing tectonic deformation, the volume and proportion of macropores increase, while the volume and proportion of mesopores initially rise and then decline, and the volume and proportion of micropores exhibit a contrasting decrease and increase, respectively. This suggests that tectonic deformation can enhance the volume of various pore types, particularly macropores. As shown in Figure 11, the specific surface area of micropores dominates in TDC, accounting for over 90%, while the specific surface areas of macropores and mesopores are significantly low, both being below 5%. From primary coal to mylonite coal, the specific surface area of micropores increases by approximately 40 m^2/g, while the increases for macropores and mesopores are both below 2 m^2/g. This suggests that tectonic deformation can enhance the specific surface area of various pore types, particularly that of micropores.

4.2 Relationship between pore structure and deformation

As the degree of coal deformation increases, the pore volume rises, and this study uses fractal theory to quantitatively describe the changes in the complexity of pore structure during deformation.

The Washburn model (Washburn, 1921) is represented in Equation 1 to analyze the pore fractal characteristics of mercury intrusion porosimetry:

$$\mathrm{Ln}(dV/dP) = (D_W - 4)\ln P + \mathrm{const} \quad (1)$$

where P is mercury intrusion pressure, MPa, V is mercury intrusion volume at pressure P, cm^3/g.

The FHH model (Frenkel-Halsey-Hill) is employed to analyze the fractal characteristics of pores in the case of low-temperature liquid N_2 adsorption method (Wang et al., 2022; Wang et al., 2024) as described in Equation 2.

$$\mathrm{Ln}V = (D_{FHH} - 3)\ln[\ln(P_0/P)] + \mathrm{const} \quad (2)$$

where V is the adsorbed liquid N_2 volume under equilibrium pressure P, cm^3/g, P_0 is the saturated vapor pressure of N_2 adsorption, MPa.

The Sierpinski model, used to analyze the fractal characteristics of pores in the case of 273 K CO_2 adsorption method (Song et al., 2017b; Wang et al., 2024), is described as Equation 3

$$\mathrm{Ln}V = (3 - D_{SIE})\ln(P - P_t) + \mathrm{const} \quad (3)$$

In the equation, P_t represents the threshold pressure, which is typically the pressure value of the first data point on the adsorption isotherm curve.

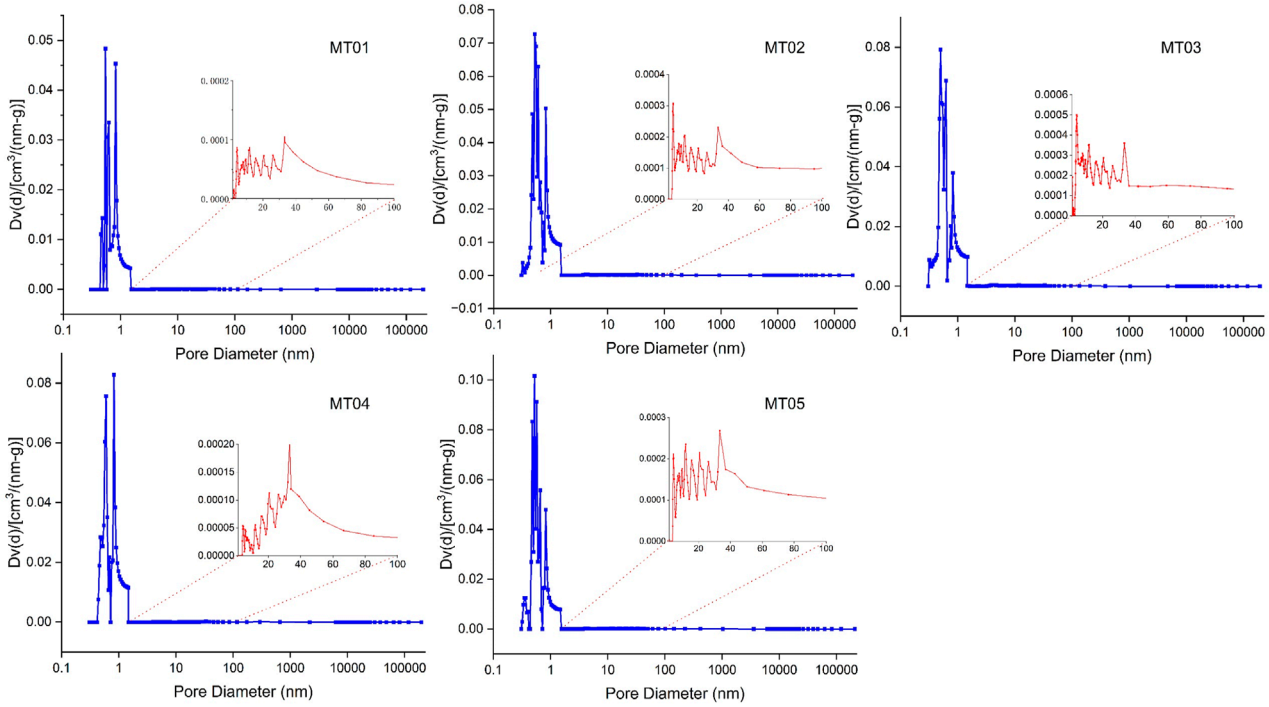

FIGURE 10
Pore size distribution characteristics.

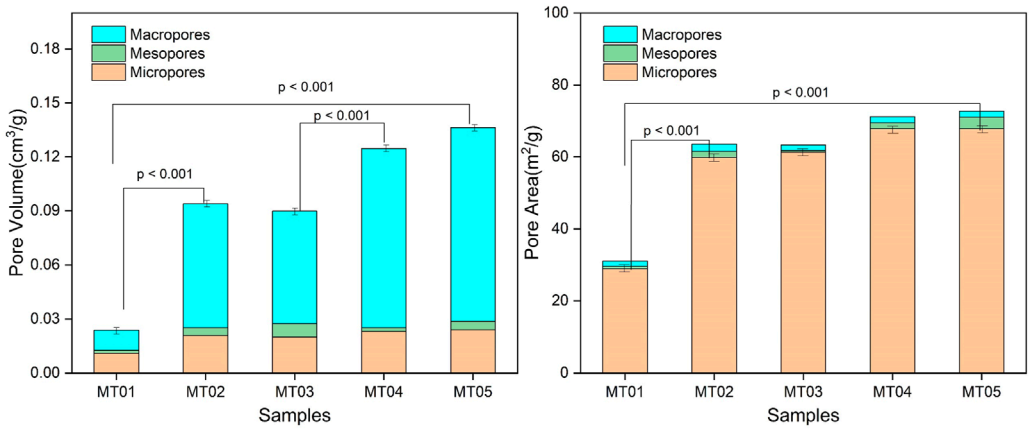

FIGURE 11
Pore volume and specific surface area of different pore size ranges. The p-values are used to calculate the volume of macropores and the specific surface area of micropores.

The calculated fractal dimensions range from 2 to 3, where a value of 2 indicates a completely smooth surface and a highly homogeneous pore structure, while a value of 3 signifies an extremely rough pore surface and a highly complex pore structure. It is evident that the different types of coal samples exhibit good fractal fitting results, with fitting coefficients ranging from 0.936 to 0.999 (Figure 12). In ductile deformed coal, the mercury intrusion porosity measurement for D_1 shows two distinct intervals, and this study selects the well-fitting data in the range of 3200–35 nm. To better understand the fractal characteristics of coal samples with varying degrees of deformation, a linear regression line with a 95% confidence interval is plotted (Figure 13). It can be observed that from pristine coal to brittle deformed coal to ductile deformed coal, D_1 exhibits a decreasing trend, particularly in ductile coal, where the D_1 value significantly declines. This indicates that as the degree of deformation increases, the macropore structure simplifies. In contrast, the D_3 value obtained from CO_2 adsorption increases with the degree of deformation, indicating that the micropore structure grows increasingly complex. The pore fractal dimension D_2 shows minimal differences among the five coal samples, suggesting that

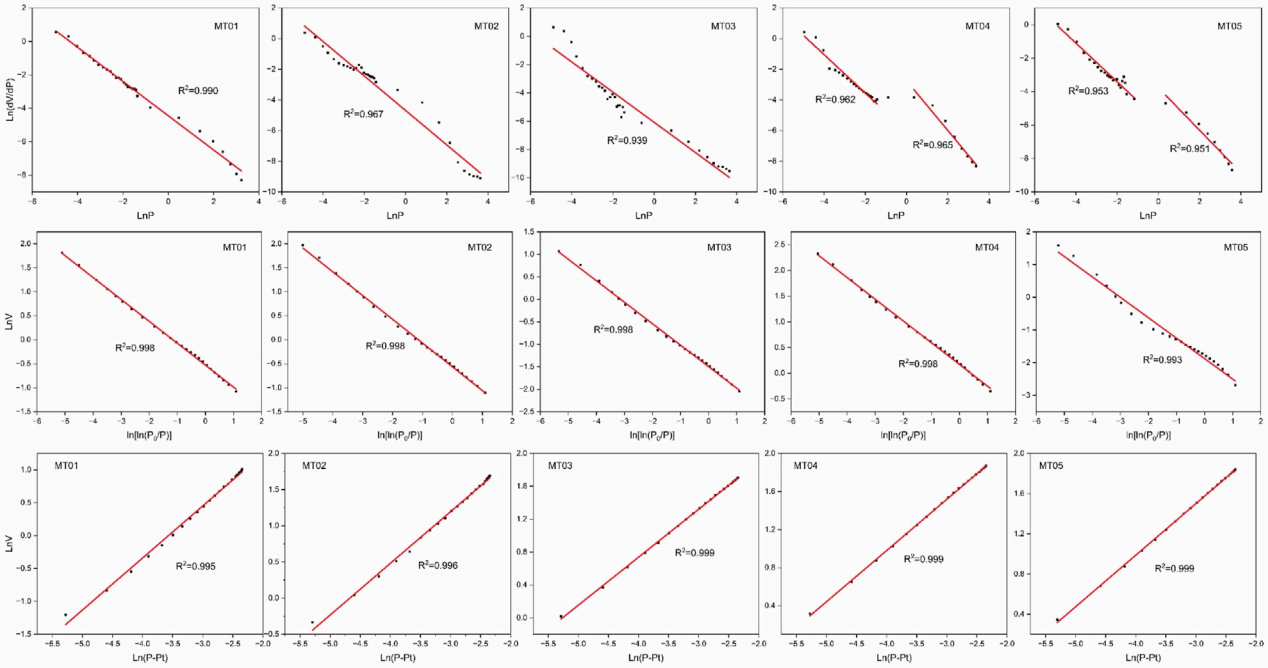

FIGURE 12
Linear fitting of different fractal models.

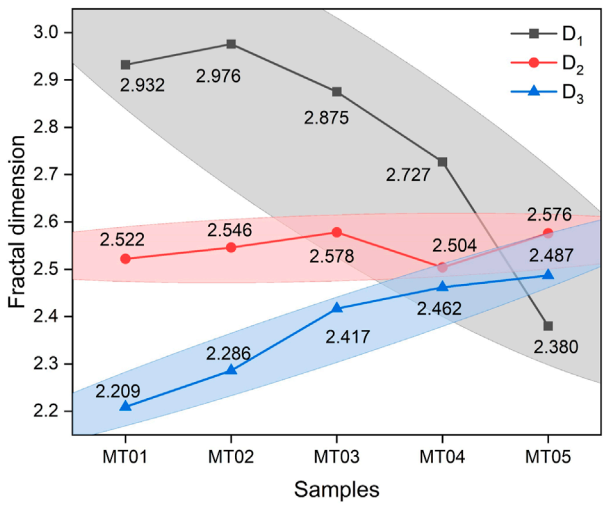

FIGURE 13
The variation of fractal dimension.

tectonic deformation has a minor effect on the complexity of the mesopore structure.

4.3 Relationship between pore structure and methane adsorption capacity

Pores are the primary pathways for gas migration and critical sites for adsorption and storage (Melnichenko et al., 2012), making pore characteristics crucial factors influencing coal's ability to adsorb methane. It is widely believed that a larger specific surface area and pore volume in coal lead to a stronger adsorption capacity (Liu and He, 2017). By combining the characterization of pore structure with the CH_4 adsorption experimental results, the influence of pore characteristics at different scales on CH_4 adsorption capacity is illustrated in Figures 14, 15. Pore volume and specific surface area show a significant positive correlation with methane adsorption capacity, particularly for micropores. Macropore volume demonstrates a significant positive correlation with methane adsorption capacity, while specific surface area does not. Neither mesopore volume nor specific surface area shows correlations, as the small mesopore volume and specific surface area in the coal samples result in limited adsorption space. Therefore, the methane adsorption capacity of coal samples in this region is primarily influenced by micropore volume and specific surface area, along with macropore volume, with minimal correlation to mesopores.

Based on previous research on the adsorption characteristics and controlling factors of coalbed methane, methane is primarily stored on the pore surfaces of coal through adsorption, with the key factor for methane adsorption capacity in coal reservoirs being its surface area (Moore, 2012; Liu and He, 2017). Micropores account for the vast majority of the total specific surface area, suggesting that micropore structure may be the main factor influencing methane adsorption capacity. Additionally, by comparing the relationship between methane adsorption capacity and pore characteristics, it is likely that the methane adsorption capacity of coal is influenced by both micropore volume and total pore volume. In this study, macropore volume demonstrates a strong correlation with methane

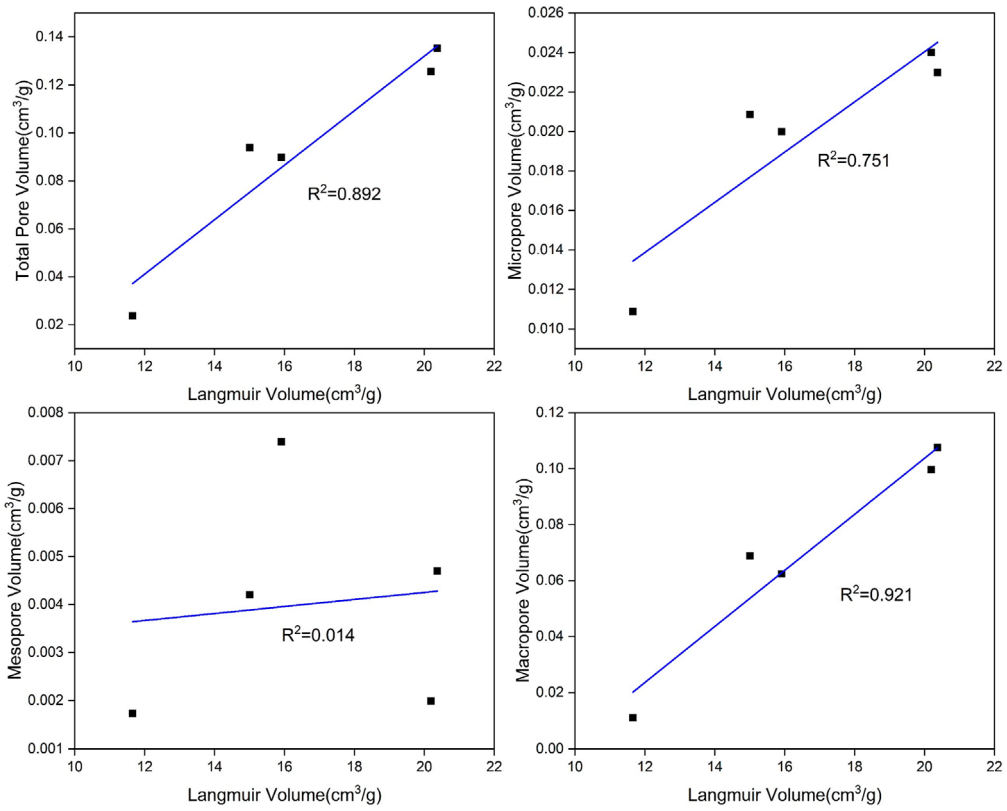

FIGURE 14
Relationship between the measured Langmuir volume a with different-scale pore volume.

adsorption capacity, while specific surface area does not exhibit any correlation. This is because the trend of macropore volume changes is consistent with that of micropores across different degrees of coal deformation, causing the influence of micropores on methane adsorption capacity to be overshadowed by macropores. Although the macropore volume in mylonite coal is ten times that of pristine coal, the methane adsorption capacity increases by less than twofold, underscoring that micropores (rather than macropores) remain the dominant contributors to adsorption. This aligns with our LTNA and CO_2 adsorption data showing a 40 m^2/g increase in micropore-specific surface area in deformed samples. Therefore, the methane adsorption capacity in this study is primarily influenced by the characteristics of the micropore structure, with mylonitic and brittle deformed coals enhancing their methane adsorption capacity through increases in micropore volume and specific surface area. Additionally, macropore volume positively influences coalbed methane, potentially acting as a major storage space for free methane (Lu et al., 2021).

In summary, as the coal in this region undergoes tectonic deformation from its original structure to brittle deformation, the pore structure gradually evolves, with an increase in micropore volume and specific surface area, resulting in a more complex pore structure that regulates methane adsorption. By the ductile deformation stage, the increase in micropore volume and specific surface area becomes limited; although macropore volume increases, the growth in specific surface area remains minimal, resulting in a less pronounced effect on methane adsorption, primarily providing space for free methane. Therefore, in coalbed methane development in this region, brittle deformed coal is often effective at enriching coalbed methane, making it a favorable area for development, while methane in the macropores of ductile deformed coal is more prone to dissipation, leading to gas outbursts. This aligns with the frequent gas outburst hazards in the Huaibei mining area (Jiang et al., 2010; Wang et al., 2013; Wang et al., 2014). These coals with greater risk of protrusion are usually characterised by higher iron content (Krasnovyd et al., 2023). In fact, it is possible to extract free methane from unloaded coal seams during the mining process by supplying energy to the seams to heat them up to a temperature of 35°C (Mullagaliyeva et al., 2022).

5 Conclusion

This study comprehensively characterizes the microscopic pore structure of various tectonically deformed coal samples and examines the impact of tectonic deformation on pore structure, while also assessing the influence of pore structure on methane adsorption capacity. The following conclusions are drawn.

(1) In the Huaibei mining area, coal primarily consists of micropores and macropores, with very low mesopore content. As the degree of tectonic deformation increases, the pore

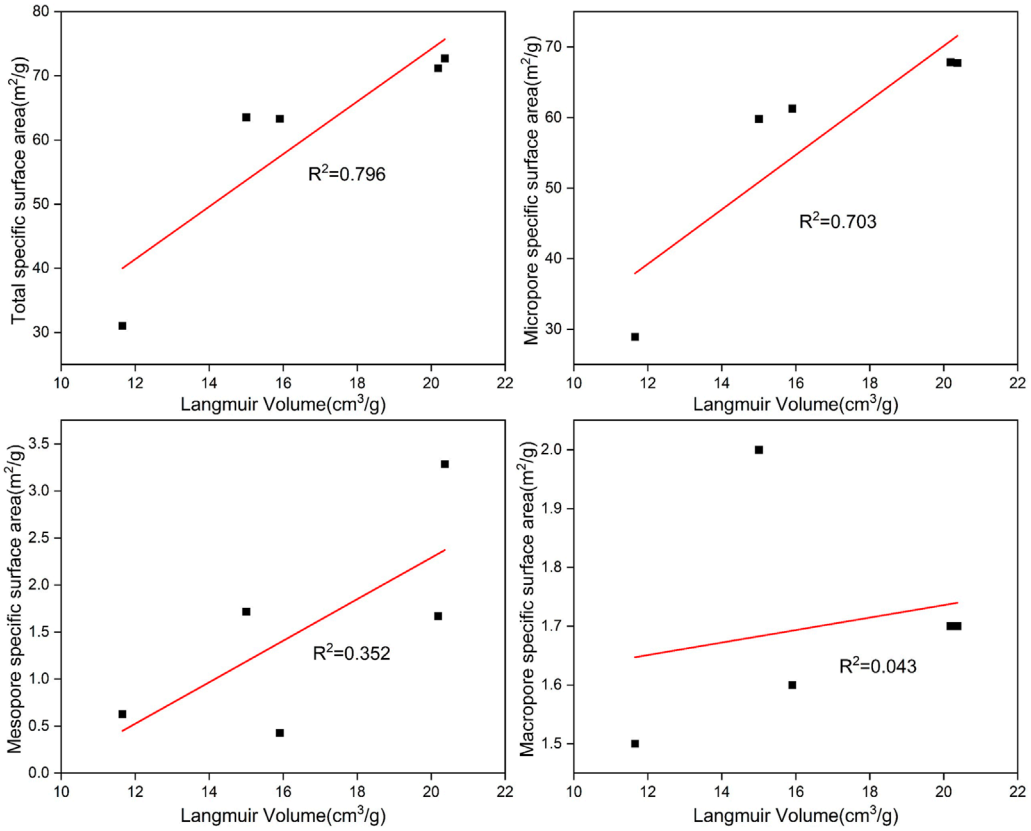

FIGURE 15
Relationship between the measured Langmuir volume a with different-scale pore SSA.

volume and specific surface area of both micropores and macropores increase, while the micropore structure becomes more complex and the macropore structure simplifies.

(2) In tectonically deformed coal, micropore volume and specific surface area are positively correlated with methane adsorption capacity, indicating that the micropore structure is the primary factor controlling methane adsorption in coal. Additionally, total pore volume and macropore volume also show a strong correlation with methane adsorption, as the volumes of micropores and macropores increase synchronously during deformation, resulting in changes in macropore volume that are similar to those in micropore volume.

(3) During tectonic deformation, the increase in micropore volume and complexity leads to a more intricate methane adsorption process, while the increase in macropore volume and simplicity results in more free methane. This may elevate the risk of gas outburst hazards during coalbed methane development.

Data availability statement

The original contributions presented in the study are included in the article/supplementary material, further inquiries can be directed to the corresponding author.

Author contributions

PW: Data curation, Methodology, Writing – review and editing, Investigation, Software, Writing – original draft, Conceptualization. YJ: Project administration, Writing – review and editing, Supervision, Funding acquisition. CR: Formal Analysis, Writing – review and editing, Funding acquisition, Project administration. GL: Visualization, Writing – review and editing, Methodology, Investigation. LX: Investigation, Writing – review and editing, Visualization. WW: Software, Writing – review and editing, Visualization. JG: Investigation, Writing – review and editing, Visualization. RC: Writing – review and editing, Investigation, Methodology.

Funding

The author(s) declare that financial support was received for the research and/or publication of this article. This research was financially supported by the National Key Research and Development Program of China (Grant Nos. 2023YFF0804300), the National Science and Technology Major Project of China (Grant No. 2016ZX05066, 2017ZX05064), and the “Climate Change: Carbon Budget and Related Issues” Strategic Priority

Research Program of the Chinese Academy of Sciences (Grant No. XDA05030100).

Conflict of interest

Author CR was employed by Qingdong Coal Mine Huaibei Min Co., Ltd.

The remaining authors declare that the research was conducted in the absence of any commercial or financial relationships that could be construed as a potential conflict of interest.

Generative AI statement

The author(s) declare that no Generative AI was used in the creation of this manuscript.

Publisher's note

All claims expressed in this article are solely those of the authors and do not necessarily represent those of their affiliated organizations, or those of the publisher, the editors and the reviewers. Any product that may be evaluated in this article, or claim that may be made by its manufacturer, is not guaranteed or endorsed by the publisher.

References

Chen, S., Tao, S., Tang, D., Xu, H., Li, S., Zhao, J., et al. (2017). Pore structure characterization of different rank coals using N2 and CO2 adsorption and its effect on CH4 adsorption capacity: a case in panguan syncline, western guizhou, China. *Energy and Fuels* 31, 6034–6044. doi:10.1021/acs.energyfuels.7b00675

Cheng, Y., and Hu, B. (2021). Main occurrence form of methane in coal:Micropore filling. *J. China Coal Soc.* 46, 2933–2948. doi:10.13225/j.cnki.jccs.2020.1214

Fu, S., Wang, L., Li, S., Ni, S., Cheng, Y., Zhang, X., et al. (2024). Re-thinking methane storage mechanism in highly metamorphic coalbed reservoirs-A molecular simulation considering organic components. *Energy* 293, 130444, doi:10.1016/j.energy.2024.130444

Fu, S., Wang, L., Li, S., Zheng, S., and Li, J. (2023). The effect of organic matter fraction extracted on micropores development degree and CH4 adsorption capacity of coal. *Gas Sci. Eng.* 110, 204870. doi:10.1016/j.jgsce.2022.204870

Fu, X., Qin, Y., Wang, G. G. X., and Rudolph, V. (2009). Evaluation of coal structure and permeability with the aid of geophysical logging technology. *Fuel* 88, 2278–2285. doi:10.1016/j.fuel.2009.05.018

He, X. X., Cheng, Y. P., Hu, B., Wang, Z. Y., Wang, C. H., Yi, M. H., et al. (2020). Effects of coal pore structure on methane-coal sorption hysteresis: an experimental investigation based on fractal analysis and hysteresis evaluation. *Fuel* 269, 117438. doi:10.1016/j.fuel.2020.117438

Hu, B., Cheng, Y., He, X., Wang, Z., Jiang, Z., Wang, C., et al. (2020). New insights into the CH_4 adsorption capacity of coal based on microscopic pore properties. *Fuel* 262, 116675. doi:10.1016/j.fuel.2019.116675

Hu, B., Cheng, Y., Wang, L., Zhang, K., He, X., and Yi, M. (2021). Experimental study on influence of adsorption equilibrium time on methane adsorption isotherm and Langmuir parameter. *Adv. Powder Technol.* 32, 4110–4119. doi:10.1016/j.apt.2021.09.015

Jiang, B., Qu, Z., Wang, G. G. X., and Li, M. (2010). Effects of structural deformation on formation of coalbed methane reservoirs in Huaibei coalfield, China. *Int. J. Coal Geol.* 82, 175–183. doi:10.1016/j.coal.2009.12.011

Ju, Y., Jiang, B., Hou, Q., and Wang, G. (2004). The new structure-genetic classification system in tectonically deformed coals and its geological significance. *J. China Coal Soc.* 29, 513–517. doi:10.3321/j.issn:0253-9993.2004.05.001

Ju, Y., Sun, Y., Tan, J., Bu, H., Han, K., Li, X., et al. (2018). The composition, pore structure characterization and deformation mechanism of coal-bearing shales from tectonically altered coalfields in eastern China. *Fuel* 234, 626–642. doi:10.1016/j.fuel.2018.06.116

Ju, Y. W., Jiang, B., Hou, Q. L., and Wang, G. L. (2005). FTIR spectroscopic study on the stress effect of compositions of macromolecular structure in tectonically deformed coals. *Spectrosc. Spectr. Analysis* 25, 1216–1220. doi:10.3321/j.issn:1000-0593.2005.08.014

Krasnovyd, S., Konchits, A., Shanina, B., Valakh, M., Yukhymchuk, V., Skoryk, M., et al. (2023). Coal from the outburst hazardous mine seams: spectroscopic study. *Min. Mineral Deposits* 17 (1), 93–100. doi:10.33271/mining17.01.093

Li, J., Huang, Q., Wang, G., and Wang, E. (2022). Influence of active water on gas sorption and pore structure of coal. *Fuel* 310, 122400. doi:10.1016/j.fuel.2021.122400

Li, S., Tang, D., Xu, H., and Yang, Z. (2012). Advanced characterization of physical properties of coals with different coal structures by nuclear magnetic resonance and X-ray computed tomography. *Comput. and Geosciences* 48, 220–227. doi:10.1016/j.cageo.2012.01.004

Li, W., Liu, H., and Song, X. (2015). Multifractal analysis of Hg pore size distributions of tectonically deformed coals. *Int. J. Coal Geol.* 144, 138–152. doi:10.1016/j.coal.2015.04.011

Li, Z., Ren, T., Li, X., Qiao, M., Yang, X., Tan, L., et al. (2023). Multi-scale pore fractal characteristics of differently ranked coal and its impact on gas adsorption. *Int. J. Min. Sci. Technol.* 33 (4), 389–401. doi:10.1016/j.ijmst.2022.12.006

Liu, B., Mohammadi, M.-R., Ma, Z., Bai, L., Wang, L., Xu, Y., et al. (2023a). Evolution of porosity in kerogen type I during hydrous and anhydrous pyrolysis: experimental study, mechanistic understanding, and model development. *Fuel* 338, 127149. doi:10.1016/j.fuel.2022.127149

Liu, J., Jiang, B., Li, M., Qu, Z., Wang, L., and Li, L. (2015). Structural control on pore-fracture characteristics of coals from Xinjing coal mine, northeastern Qinshui basin, China. *Arabian J. Geosciences* 8, 4421–4431. doi:10.1007/s12517-014-1551-3

Liu, X., and He, X. (2017). Effect of pore characteristics on coalbed methane adsorption in middle-high rank coals. *Adsorption-Journal Int. Adsorpt. Soc.* 23, 3–12. doi:10.1007/s10450-016-9811-z

Liu, X., Nie, B., Wang, W., Wang, Z., and Zhang, L. (2019). The use of AFM in quantitative analysis of pore characteristics in coal and coal-bearing shale. *Mar. Petroleum Geol.* 105, 331–337. doi:10.1016/j.marpetgeo.2019.04.021

Liu, X. F., Jia, X. Q., Liu, W., Nie, B. S., Zhang, C. P., and Song, D. Z. (2023b). Mechanical strength and porosity changes of bituminous coal induced by supercritical CO2 interactions: influence of saturation pressure. *Geoenergy Sci. Eng.* 225, 211691. doi:10.1016/j.geoen.2023.211691

Liu, Y. X., Hao, C. M., Wang, Z. Y., Xie, J. N., Zhao, W. B., Meng, F. B., et al. (2024). Micropore distribution and methane adsorption process and mechanism in bituminous coals: a molecular dynamics simulation study. *J. Environ. Chem. Eng.* 12 (2), 112139. doi:10.1016/j.jece.2024.112139

Lu, G., Wei, C., Wang, J., Meng, R., and Tamehe, L. S. (2021). Influence of pore structure and surface free energy on the contents of adsorbed and free methane in tectonically deformed coal. *Fuel* 285, 119087. doi:10.1016/j.fuel.2020.119087

Mastalerz, M., He, L., Melnichenko, Y. B., and Rupp, J. A. (2012). Porosity of coal and shale: insights from gas adsorption and SANS/USANS techniques. *Energy and Fuels* 26, 5109–5120. doi:10.1021/ef300735t

Melnichenko, Y. B., He, L., Sakurovs, R., Kholodenko, A. L., Blach, T., Mastalerz, M., et al. (2012). Accessibility of pores in coal to methane and carbon dioxide. *Fuel* 91, 200–208. doi:10.1016/j.fuel.2011.06.026

Moore, T. A. (2012). Coalbed methane: a review. *Int. J. Coal Geol.* 101, 36–81. doi:10.1016/j.coal.2012.05.011

Mullagaliyeva, L. F., Baimukhametov, S. K., Portnov, V. S., and Yurov, V. M. (2022). On the issue of thermal destruction of coal matter. *Eng. J. Satbayev Univ.* 144 (1), 57–61. doi:10.51301/ejsu.2022.i1.09

Pan, J., Niu, Q., Wang, K., Shi, X., and Li, M. (2016). The closed pores of tectonically deformed coal studied by small-angle X-ray scattering and liquid nitrogen adsorption. *Microporous Mesoporous Mater.* 224, 245–252. doi:10.1016/j.micromeso.2015.11.057

Pan, J., Wang, S., Ju, Y., Hou, Q., Niu, Q., Wang, K., et al. (2015). Quantitative study of the macromolecular structures of tectonically deformed coal using high-resolution transmission electron microscopy. *J. Nat. Gas Sci. Eng.* 27, 1852–1862. doi:10.1016/j.jngse.2015.11.012

Qu, Z., Jiang, B., Wang, J., and Li, M. (2017). Study of nanopores of tectonically deformed coal based on liquid nitrogen adsorption at low temperatures. *J. Nanosci. Nanotechnol.* 17, 6566–6575. doi:10.1166/jnn.2017.14470

Sing, K. S. W., Everett, D. H., Haul, R. A. W., Moscou, L., Pierotti, R. A., Rouquerol, J., et al. (1985). Reporting physisorption data for gas solid systems with special reference to the determination of surface-area and porosity (recommendations 1984). *Pure Appl. Chem.* 57 (4), 603–619. doi:10.1351/pac198557040603

Song, Y., Jiang, B., and Lan, F. (2019). Competitive adsorption of CO2/N2/CH4 onto coal vitrinite macromolecular: effects of electrostatic interactions and oxygen functionalities. *Fuel* 235, 23–38. doi:10.1016/j.fuel.2018.07.087

Song, Y., Jiang, B., Li, F., and Liu, J. (2017a). Structure and fractal characteristic of micro- and meso-pores in low, middle-rank tectonic deformed coals by CO2 and N2 adsorption. *Microporous Mesoporous Mater.* 253, 191–202. doi:10.1016/j.micromeso.2017.07.009

Song, Y., Jiang, B., Li, M., Liu, J.-G., Cheng, G.-X., and Tang, Z. (2017b). Nano-porous structural evolution and tectonic control of low-medium metamorphic tectonically deformed coals-taking suxian mine field as an example. *J. Nanosci. Nanotechnol.* 17, 6083–6095. doi:10.1166/jnn.2017.14476

Thommes, M., Kaneko, K., Neimark, A. V., Olivier, J. P., Rodriguez-Reinoso, F., Rouquerol, J., et al. (2015). Physisorption of gases, with special reference to the evaluation of surface area and pore size distribution (IUPAC Technical Report). *Pure Appl. Chem.* 87, 1051–1069. doi:10.1515/pac-2014-1117

Wang, H., Wang, L., Cheng, Y., and Zhou, H. (2013). Characteristics and dominant controlling factors of gas outburst in Huaibei coalfield and its countermeasures. *Int. J. Min. Sci. Technol.* 23, 591–596. doi:10.1016/j.ijmst.2013.07.019

Wang, H., Wang, L., Zheng, S., Sun, Y., Shen, S., and Zhang, X. (2024). Research on coal matrix pore structure evolution and adsorption behavior characteristics under different thermal stimulation. *Energy* 287, 129677. doi:10.1016/j.energy.2023.129677

Wang, L., Cheng, Y.-p., An, F.-h., Zhou, H.-x., Kong, S.-l., and Wang, W. (2014). Characteristics of gas disaster in the Huaibei coalfield and its control and development technologies. *Nat. Hazards* 71, 85–107. doi:10.1007/s11069-013-0901-x

Wang, L., Long, Z., Song, Y., and Qu, Z. (2022). Supercritical CO_2 adsorption and desorption characteristics and pore structure controlling mechanism of tectonically deformed coals. *Fuel* 317, 123485. doi:10.1016/j.fuel.2022.123485

Wang, Y., Zhu, Y., Liu, S., and Zhang, R. (2016). Pore characterization and its impact on methane adsorption capacity for organic-rich marine shales. *Fuel* 181, 227–237. doi:10.1016/j.fuel.2016.04.082

Washburn, E. W. (1921). The dynamics of capillary flow. *Phys. Rev.* 17, 273–283. doi:10.1103/physrev.17.273

Xu, R., Li, H., Guo, C., and Hou, Q. (2014). The mechanisms of gas generation during coal deformation: preliminary observations. *Fuel* 117, 326–330. doi:10.1016/j.fuel.2013.09.035

Yang, Y., Liu, S., Zhao, W., and Wang, L. (2019). Intrinsic relationship between Langmuir sorption volume and pressure for coal: experimental and thermodynamic modeling study. *Fuel* 241, 105–117. doi:10.1016/j.fuel.2018.12.008

Yao, Y., Liu, D., Tang, D., Tang, S., Huang, W., Liu, Z., et al. (2009). Fractal characterization of seepage-pores of coals from China: an investigation on permeability of coals. *Comput. and Geosciences* 35, 1159–1166. doi:10.1016/j.cageo.2008.09.005

Yu, K., Ju, Y., Qian, J., Qu, Z., Shao, C., Yu, K., et al. (2018a). Burial and thermal evolution of coal-bearing strata and its mechanisms in the southern North China Basin since the late Paleozoic. *Int. J. Coal Geol.* 198, 100–115. doi:10.1016/j.coal.2018.09.007

Yu, S., Bo, J., and Jie-gang, L. (2017). Nanopore structural characteristics and their impact on methane adsorption and diffusion in low to medium tectonically deformed coals: case study in the Huaibei coal field. *Energy and Fuels* 31, 6711–6723. doi:10.1021/acs.energyfuels.7b00512

Yu, S., Bo, J., Pei, S., and Wu, J. (2018b). Matrix compression and multifractal characterization for tectonically deformed coals by Hg porosimetry. *Fuel* 211, 661–675. doi:10.1016/j.fuel.2017.09.070

Yuan, J., Zhang, H., Guo, Y., and Cai, N. (2017). Thermodynamic properties of high-rank tectonically deformed coals during isothermal adsorption. *Arabian J. Geosciences* 10, 278. doi:10.1007/s12517-017-3066-1

Zhang, C., Xu, J., Peng, S., Li, Q., and Yan, F. (2019a). Experimental study of drainage radius considering borehole interaction based on 3D monitoring of gas pressure in coal. *Fuel* 239, 955–963. doi:10.1016/j.fuel.2018.11.092

Zhang, C., Xu, J., Peng, S., Li, Q., Yan, F., and Chen, Y. (2018). Dynamic behavior of gas pressure and optimization of borehole length in stress relaxation zone during coalbed methane production. *Fuel* 233, 816–824. doi:10.1016/j.fuel.2018.06.132

Zhang, F., Jiang, J. Y., Wang, C. H., Cheng, Y. P., Dong, X. B., and Wu, J. (2025). Influence of components on methane micropore filling capacity of low-rank coal. *Powder Technol.* 449, 120363. doi:10.1016/j.powtec.2024.120363

Zhang, K. Z., Cheng, Y. P., Li, W., Hao, C. M., Hu, B., and Jiang, J. Y. (2019b). Microcrystalline characterization and morphological structure of tectonic anthracite using XRD, liquid nitrogen adsorption, mercury porosimetry, and micro-CT. *Energy and Fuels* 33, 10844–10851. doi:10.1021/acs.energyfuels.9b02756

Zhang, R., and Liu, S. M. (2017). Experimental and theoretical characterization of methane and CO_2 sorption hysteresis in coals based on Langmuir desorption. *Int. J. Coal Geol.* 171, 49–60. doi:10.1016/j.coal.2016.12.007

Zheng, S., An, Y. F., Lai, C. K., Wang, H. Z., and Li, Y. F. (2021). Genesis of high-Mg adakites in the southeastern margin of north China craton: geochemical and U-Pb geochronological perspectives. *Front. Earth Sci.* 9. doi:10.3389/feart.2021.731233

Zhou, S., Liu, D., Cai, Y., Karpyn, Z., and Yao, Y. (2018). Comparative analysis of nanopore structure and its effect on methane adsorption capacity of Southern Junggar coalfield coals by gas adsorption and FIB-SEM tomography. *Microporous Mesoporous Mater.* 272, 117–128. doi:10.1016/j.micromeso.2018.06.027

Zhu, J., Zhang, Y., Zhang, R., Zhang, B., Tang, J., and He, F. (2020). Surface fractal dimensions as a characterization parameter for methane adsorption-induced coal strains. *Arabian J. Geosciences* 13, 997. doi:10.1007/s12517-020-06024-z

Zou, M., Wei, C., Huang, Z., and Wei, S. (2015). Porosity type analysis and permeability model for micro-trans-pores, meso-macro-pores and cleats of coal samples. *J. Nat. Gas Sci. Eng.* 27, 776–784. doi:10.1016/j.jngse.2015.09.025